J. Fluid Mech. (2005), *vol.* 532, *pp.* 165–189. © 2005 Cambridge University Press
doi:10.1017/S0022112005003988 Printed in the United Kingdom

Stress gradient balance layers and scale hierarchies in wall-bounded turbulent flows

By P. FIFE[1], T. WEI[2], J. KLEWICKI[2] AND P. McMURTRY[2]

[1]Department of Mathematics, University of Utah, Salt Lake City, UT 84112, USA
[2]Department of Mechanical Engineering, University of Utah, Salt Lake City, UT 84112, USA

(Received 23 March 2004 and in revised form 28 December 2004)

Steady Couette and pressure-driven turbulent channel flows have large regions in which the gradients of the viscous and Reynolds stresses are approximately in balance (stress gradient balance regions). In the case of Couette flow, this region occupies the entire channel. Moreover, the relevant features of pressure-driven channel flow throughout the channel can be obtained from those of Couette flow by a simple transformation. It is shown that stress gradient balance regions are characterized by an intrinsic hierarchy of 'scaling layers' (analogous to the inner and outer domains), filling out the stress gradient balance region except for locations near the wall. The spatial extent of each scaling layer is found asymptotically to be proportional to its distance from the wall.

There is a rigorous connection between the scaling hierarchy and the mean velocity profile. This connection is through a certain function $A(y^+)$ defined in terms of the hierarchy, which remains $O(1)$ for all y^+. The mean velocity satisfies an exact logarithmic growth law in an interval of the hierarchy if and only if A is constant. Although A is generally not constant in any such interval, it is arguably almost constant under certain circumstances in some regions. These results are obtained completely independently of classical inner/outer/overlap scaling arguments, which require more restrictive assumptions.

The possible physical implications of these theoretical results are discussed.

1. Introduction

Boundary-layer and pressure-driven or shear-driven channel flows transition to turbulence at sufficiently high Reynolds numbers.† Within the turbulent regime, numerous empirical observations, e.g. Gad-el-Hak & Bandyopadhyay (1994), indicate that many of the statistical properties of these flows are similar, even though they possess different driving mechanisms. This apparent statistical similarity supports claims for an underlying similarity in the dynamical structure of the turbulence as well. In the case of pressure- and shear-driven turbulent flows, structural similarity will be one of the themes in this paper.

Theoretical approaches to the description of the mean velocity profile in both shear- and pressure-driven flows often start by assuming a mathematical structure formally describing behaviour in two separate scaling regions – the inner, where the law of

† This paper will primarily employ the so-called Kármán number, $\delta^+ = \delta u_\tau/\nu$, where δ is the boundary-layer thickness or channel half-height, ν is the kinematic viscosity, u_τ is the friction velocity ($\equiv\sqrt{\tau_{wall}/\rho}$), τ_{wall} is the surface shear stress, and ρ mass density.

the wall holds, and the outer, where the defect law governs the flow. Subsequent analyses (classical and modern) then typically propose the existence of a region of overlap where both representations are valid. Such traditional methodologies have their origin in the work of Izakson (1937) and Millikan (1939). (Gill (1968) rightly showed that in addition to assuming the existence of an overlap region, one must assume appropriate maximal rates of growth, as the outer variable approaches 0, of the discrepancy between the outer approximation and the true solution, and similarly with the inner approximation as that variable approaches ∞.)

This traditional framework constitutes the basis for a number of the theoretical approaches attempting to describe the physical behaviours of wall turbulence. For example, this inner/outer/overlap structure promotes the notion that the logarithmic region of the mean profile is an inertial sublayer in physical space (e.g. Tennekes & Lumley 1972), and has been employed in constructing descriptions of the Reynolds normal and shear stresses (Monin & Yaglom 1971; Panton 1997, 2005). More generally, the classical train of thought has been at the foundation of a great many theoretical treatments of wall-bounded turbulence in the last decade or so (Afzal 1993, 2001*a*, *b*; George & Castillo 1997; Panton 1997, 2005; Buschmann & Gad-el-Hak 2003*a*, *b*).

For the mean velocity profile, the hypothesized overlap region is traditionally handled by matching the velocity gradient, as simultaneously represented by the inner and outer functions (e.g. Tennekes & Lumley 1972). In this way a logarithmic velocity profile is obtained. There is, however, a rational basis for questioning the logic of the methodology. First, while generic prototypical two-scale problems with an overlap region arising in other contexts lead to the solution being constant in the overlap domain, such constancy in the present case is not acceptable. It is known that the mean velocity profile is a strictly increasing function of distance from the wall. Secondly, it is straightforward to construct quite arbitrary mathematical functions with inner and outer scaling regions in which the traditional forms for the corresponding approximations are satisfied, but which have no overlap zone of joint validity, and no logarithmic profile. Thirdly, while the overlap ideas often constitute an empirically convincing framework for organizing data, a lucid description of the dynamical structure underlying such a region has yet to emerge. The foundation provided in Wei *et al.* (2005), upon which the present analysis builds, avoids the ambiguity associated with the overlap hypothesis by basing its analysis directly on the scaling properties of the mean differential statement of Newton's second law.

To summarize, there is reason to question whether the pair of hypotheses, (*i*) an overlap zone exists, and (*ii*) the profile is strictly increasing, forms a reasonable basis for a derivation (see the further discussion in Wei *et al.* 2005). One goal of the present work is to construct an approach to the derivation of features of the mean velocity and Reynolds stress profiles that is distinct from the classical one. This approach seeks to employ a train of reasoning beginning with credible hypotheses that are disconnected from the phenomenon to be explained.

The present paper greatly expands on Wei *et al.* (2005). Specifically, the arguments in that paper reveal that while Reynolds-number dependencies in the mean velocity profile (using inner scaling) appear only very subtly, the Reynolds-number-dependent behaviour of the terms in the mean momentum balance are both clearly evident in existing data, and derivable from the equations of motion. From these new results, we are also led to conclusions regarding flow structure that are contrary to a number of well-established notions within the turbulent wall-flow literature. Notable among the latter are (*i*) that viscous forces are only comparable to turbulent

inertia in the buffer layer and below (say $y^+ = yu_\tau/\nu$ less than about 30), (*ii*) the aforementioned correspondence between a logarithmic mean profile and an inertial sublayer-like structure in physical space, and (*iii*) the exclusivity of the inner and outer scales with regard to describing the behaviour of mean momentum transport and its Reynolds-number dependence. The new assertions, contrary to those just listed, are corroborated by the highest quality data available (Zagarola & Smits 1997; Moser, Kim & Mansour 1999; DeGraaff & Eaton 2000; McKeon *et al.* 2004), as well as via multiscale analyses under a minimal set of well-founded assumptions. At the heart of this theory is the actual balance of terms in the mean momentum equation (as opposed to the mean profile and stress-based interpretations, as in Tennekes & Lumley 1972; Hinze 1975; Townsend 1976; Panton 1990; Pope 2000). Resulting from this effort is the identification of a layer structure for channel flows, and by extension for boundary-layer and pipe flows, and that is well-founded in the mathematical representation of mean flow dynamics. A primary element of this layer structure is the so-called stress gradient balance layer.

As the name implies, a stress gradient balance layer exists when there is a balance between the viscous and Reynolds stress gradient terms in the mean momentum equation (see (2.1) below). In boundary layers, pipes and channels, the stress gradient balance layers extend from the edge of the viscous sublayer ($y^+ \approx 3$) to an inner normalized wall-normal position that is proportional to the square root of the global Reynolds number, $\sqrt{\delta^+}$. As is readily apparent, at high Reynolds numbers, the position $y^+ \sim \sqrt{\delta^+}$ extends well into the traditional logarithmic layer of the mean profile. In terms of non-normalized physical dimension, this layer thickness is given by the intermediate length, $\sqrt{\delta\nu/u_\tau}$ (Long & Chen 1981; Afzal 1984; Sreenivasan & Sahay 1997). These scaling behaviours find universal support from existing empirical data, and have been theoretically derived through the aforementioned multiscale analyses of the equations of motion. In addition to showing the necessity of this intermediate scaling for describing the mean momentum field in wall-bounded flows, there is evidence that a mean profile having features of a logarithmic profile can occur, entirely owing to the flow physics intrinsic to the stress gradient balance layer, i.e. independent of any flow structure requiring description via inner/outer overlap ideas (Wei *et al.* (2005), together with the much stronger argument and more exact definition of these features given in the present paper).

In this paper, these basic results are extended to show that stress gradient balance layers have a mathematical structure composed of a hierarchy of length scales. The picture of only two scaling regions – inner and outer – with their attendant analysis, is shown with considerable rigour to be inadequate for a full understanding. It is argued here, through rescaling arguments, that the mathematical structure of the flow involves a continuum of length scales, in a sense to be explained below. Each has its own 'scaling layer', with characteristic length asymptotically proportional to distance from the wall as that distance, in wall coordinates, increases. In all, this continuum of layers serves to connect the traditional 'outer' region with a region close to the 'inner' one. Although the analysis here is sound, the relationship between this mathematical structure and the instantaneous motions in the flow is, at this time, speculative. Furthermore, while there may be connections between the hierarchical scalings formally admitted by the mean dynamical equation (as shown herein) and the hierarchical eddy structures posed in Townsend's attached eddy hypothesis (Townsend 1976; Perry & Chong 1982; Perry & Marusic 1995), such connections await future verification. Possible implications of the scale hierarchy identified by the present effort, relative to flow physics and hierarchy-based models, are briefly discussed in § 5.

The scale hierarchy revealed herein also has consequences relating to the functional form of the mean velocity profile. Specifically, a rigorous connection is established between a certain well-defined characteristic function $A(y^+)$ associated with the hierarchy, and the mean velocity profile. The function A is guaranteed to take on $O(1)$ values for all y^+ in the hierarchy, and to be constant in any interval if and only if the profile is logarithmic in that same interval. If A is almost constant (and there are indications when this may be the case), then the profile is close to being logarithmic. Although it is generally not constant, an argument pointing to its constancy in certain regions in the limit as $Re \to \infty$ is given in § 3.5.2. For finite Re, other functions such as certain power laws could be accommodated, and certainly Re-dependence as well. Nevertheless, it is the firmest theoretical basis yet found for a generalized logarithm-type growth, and is entirely independent of the classical arguments for logarithmic growth based on an overlap hypothesis.

Finally, the general location where the hierarchy begins can be predicted, and coincides roughly with the empirical onset of the traditional logarithmic part of the velocity profile. Specifically, this location is theoretically shown to be identified with where the derivative of the Reynolds stress, namely $(\mathrm{d}/\mathrm{d}y^+)\langle uv\rangle^+$, is in a range near -0.01, with its second derivative positive. This implies that the start of the log profile is near $y^+ = 30$.

The analysis in this paper proceeds directly from the mean momentum balance equation, whose terms represent the different forces acting in the fluid. This is contary to traditional practice, in which the integrated form of that equation is used, the terms representing stresses. The two forms are equivalent, but the unintegrated form more directly displays the flow information (scaling structure) that is of primary interest here (see figure 1. (In other analogous settings, compare the velocity *vs.* vorticity forms of the flow equations; although equivalent, they convey flow information in different ways, and are therefore useful for different purposes.)

The theoretical and empirical evidence to date provide good reasons for exploring further the physical and mathematical properties of stress gradient balance layers. In this regard, consideration of purely shear-driven flow (turbulent Couette flow) is especially relevant. As will be shown, the properties of turbulent Couette flow are exclusively derived via stress gradient balance layer dynamics. Moreover, the scaling properties of turbulent channel flow can be derived from those of Couette flow by a simple transformation. The latter therefore provides a particularly useful and general context for educing the essential characteristics of stress gradient balance layer dynamics, which is a primary objective of this paper. The analysis of Couette flow (§ 3) and turbulent channel flow (§ 4) will be preceded (§ 2) by a review of existing results relating to the structure of pressure-driven turbulent flow in a channel, and followed (§ 5) by a discussion of the implications of the major results.

2. Momentum balance layer structure of turbulent channel flow

This section gives a brief recapitulation of known results about the structure of the mean momentum balance in turbulent channel flow. Its intent, in part, is to provide a context for comparisons with turbulent Couette flow, which will be the primary topic of the analysis in § 3.

In this and subsequent sections, the time-averaged form of the axial momentum balance will be considered for statistically stationary, fully developed flow in a channel of height 2δ. As is customary, the mean velocity, $U(y)$, is in the x-direction with the transverse coordinate, y, extending from its origin at the lower wall to the channel

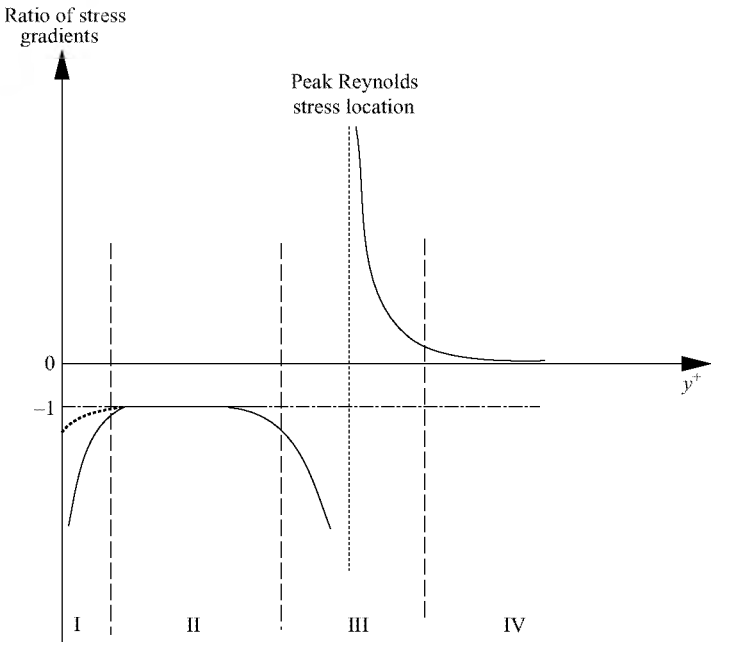

FIGURE 1. Sketch of the four layers of turbulent channel flow at a fixed Reynolds number; layer I is the inner viscous/pressure gradient balance layer, layer II is the stress gradient balance layer, layer III is the viscous/pressure gradient balance mesolayer and layer IV is the Reynolds stress/pressure gradient balance layer. Note layer I in the zero pressure gradient turbulent boundary layer is different from that of channel and pipe flow in that all of the terms in the boundary-layer equation are zero at the wall.

centreline at $y = \delta$. In the case of pressure driven flow in the channel, the inner normalized differential statement of Newton's second law is

$$0 = \frac{1}{\delta^+} + \frac{\mathrm{d}^2 U^+}{\mathrm{d}y^{+2}} - \frac{\mathrm{d}\langle uv\rangle^+}{\mathrm{d}y^+}. \tag{2.1}$$

It is crucial to recognize, in different parts of the flow, the relative orders of magnitude, as $\delta^+ \to \infty$, of the three terms in (2.1). The only possibilites are: (*i*) the three dynamical effects are, in order of magnitude, in balance, or (*ii*) two terms are in balance with the third much smaller. The various possibilities can be gauged by the ratio of two of the three terms in (2.1): the gradient of the viscous stress and the gradient of the Reynolds stress, i.e. $|\mathrm{d}^2 U^+/\mathrm{d}y^{+2}/\mathrm{d}\langle uv\rangle^+/\mathrm{d}y^+|$.

Consideration of the balance of terms in (2.1) reveals the layer structure shown schematically in figure 1 (from Wei *et al.* 2005). This figure depicts a thin sublayer ($0 \leqslant y^+ \leqslant 3$) where the mean pressure gradient and the viscous stress gradient dominate the balance equation (layer I, the inner viscous/pressure gradient layer). Outside this thin layer is a region defined by a nearly perfect balance between the viscous and Reynolds stress gradients (layer II, the Reynolds stress/viscous stress gradient balance layer). The thickness of this stress gradient balance layer exhibits a clear Reynolds-number dependence, extending well into the traditionally accepted logarithmic region of the mean velocity profile at sufficiently large Reynolds number. Near the location, y_m^+, of maximum Reynolds stress, the viscous force and pressure gradient are, once again, nearly in balance (layer III, the viscous/pressure gradient mesolayer). Around

y_m^+, the gradient of the viscous stress is much larger than the gradient of the Reynolds stress, although $|\langle uv\rangle^+| \gg \mathrm{d}U^+/\mathrm{d}y^+$. For greater distances from the wall, the Reynolds stress gradient has changed sign and the viscous stress gradient becomes much smaller than either the Reynolds stress gradient or the mean pressure gradient terms. In this region (layer IV, the Reynolds stress/pressure gradient balance layer), the Reynolds stress and pressure gradients are essentially in balance.

As is readily apparent, this layer structure constitutes a considerable departure from the sub-, buffer, logarithmic, wake layer structure typically ascribed to turbulent wall-flows. The detailed scaling behaviours associated with the layer structure depicted in figure 1 are revealed in detail by Wei *et al.* (2005). In what follows, the structure of a turbulent flow that is entirely characterized by stress gradient balance layer dynamics (i.e. Couette flow) is contrasted with, yet found to be intimately connected to, the pressure-driven channel flow.

3. Scaling analysis of turbulent Couette flow

This section is devoted to an investigation of steady turbulent Couette flow, via the averaged equation of (streamwise) momentum balance and concepts from multiscale analysis. Specifically, implications relating to the scaling-layer structure of the flow and the behaviour of the mean velocity $U^+ = U/u_\tau$ and Reynolds stress $T^+ = -\langle uv\rangle/u_\tau^2$ profiles across the channel will be explored.

The two channel walls are situated at positions $y = 0$ and $y = 2\delta$. The lower one is stationary and the upper one is in steady motion. The dimensionless inner scaled half-width of the channel is denoted by $\delta^+ = u_\tau\delta/\nu$. The parameter $\epsilon = 1/\sqrt{\delta^+}$, which is assumed to be small, will figure prominently in the various scalings. The traditional inner and outer scaled distances from the lower wall are y^+ and $\eta = \epsilon^2 y^+$, respectively. The latter is simply the physical distance from the lower wall, normalized by δ. The centreline is at $\eta = 1$, i.e. $y^+ = \epsilon^{-2} = \delta^+$. A major conclusion will be that the designation of coordinates as being either 'inner' or 'outer' may be misleading, because they represent only the extreme ends of a spectrum of scaled distances. In fact, the theoretical basis for judging the relevance of using y^+ near the wall and η near the centreline is extended here to derive the existence of the intermediate scaling regions. The new intermediate scalings therefore enjoy a theoretical foundation as firm as that of the traditional inner and outer regions.

3.1. *The averaged momentum balance equations*

The averaged equation of streamwise momentum balance for steady turbulent Couette flow expresses an exact balance between the transverse gradients of the viscous and Reynolds stresses:

$$\frac{\mathrm{d}^2U^+}{\mathrm{d}y^{+2}} + \frac{\mathrm{d}T^+}{\mathrm{d}y^+} = 0. \tag{3.1}$$

The variables U^+ and T^+ satisfy the following boundary conditions at $y^+ = 0$:

$$T^+(0) = \frac{\mathrm{d}T^+}{\mathrm{d}y^+}(0) = U^+(0) = 0; \quad \frac{\mathrm{d}U^+}{\mathrm{d}y^+}(0) = 1. \tag{3.2}$$

In terms of η, (3.1) becomes

$$\epsilon^2\frac{\mathrm{d}^2U^+}{\mathrm{d}\eta^2} + \frac{\mathrm{d}T^+}{\mathrm{d}\eta} = 0. \tag{3.3}$$

At the centreline, there are boundary conditions

$$\frac{\mathrm{d}T^+}{\mathrm{d}\eta} = \frac{\mathrm{d}^2U^+}{\mathrm{d}\eta^2} = 0 \quad \text{at } \eta = 1. \tag{3.4}$$

Beyond $\eta = 1$, U^+ and T^+ can be continued by symmetry considerations: U^+ is odd and T^+ is even with respect to their values at the centreline (see the details following (3.11)). This means, for example, that the centreline velocity U_c^+ is equal to $V^+/2$, where V^+ is the inner normalized velocity of the upper wall.

Equation (3.1) can be integrated with use of (3.2) to obtain

$$\frac{\mathrm{d}U^+}{\mathrm{d}y^+} - 1 + T^+ = 0; \tag{3.5}$$

or in terms of variable η,

$$\epsilon^2 \frac{\mathrm{d}U^+}{\mathrm{d}\eta} - 1 + T^+ = 0. \tag{3.6}$$

The 'outer approximation' is found by setting $\epsilon = 0$ in (3.6), which yields

$$T^+(\eta) = 1. \tag{3.7}$$

Alternatively, we can define a scaled Reynolds stress $\hat{T}(\eta)$ by

$$T^+ = T_m^+ + \epsilon^2 \hat{T}, \tag{3.8}$$

where $T_m^+ = T_{\eta=1}^+$, and thereby rewrite (3.3) as

$$\frac{\mathrm{d}^2U^+}{\mathrm{d}\eta^2} + \frac{\mathrm{d}\hat{T}}{\mathrm{d}\eta} = 0. \tag{3.9}$$

This, together with the observation from (3.4) that both terms in (3.9) vanish at $\eta = 1$, expresses a balance between rescaled forces and therefore suggests that the rescaling in question (U^+ and $\hat{T}$ as functions of η) is the correct one in the outer regime. In § 3.4.6, a stronger corroboration of this conclusion will be presented.

To reiterate, scaling arguments imply that near the centreline, (3.7) holds to lowest order as $\epsilon \to 0$, $\hat{T}(\eta)$ is a regular function (i.e. its derivatives with respect to η up to some finite order are bounded depending on ϵ), and (3.9) holds to next order, again as $\epsilon \to 0$. Some of these conclusions are well known (e.g. Panton 2005); they are given here as an illustrative example of the methodology used in this paper to reveal a hierarchy of layers (§ 3.4.3).

Since the outer solution (3.7) does not satisfy the boundary condition (3.2) at the lower wall, it cannot be uniformly valid; there is a thin layer near that wall where the outer scaling gives way to the inner scaling. More precisely, it will be shown, in fact, that a whole hierarchy of scalings are appropriate, forming a transition between the outer and the inner regions. First, however, a more detailed comparison with channel flow will be provided, as well as some features of the flow near the centreline.

3.2. *Comparative formulation of turbulent channel flow*

In this section, a digression is made in order (*a*) to make pertinent comparisons between Couette and channel flow, and (*b*) to introduce a transformation, (3.12), whose generalizations will lead to far-reaching implications for the profiles of both Couette and channel flows.

Physically, pressure-driven turbulent channel flow differs from Couette flow in the nature of the force driving the flow. A pressure gradient, present throughout the flow,

provides that forcing in place of the differential motion of the upper and lower walls characteristic of Couette flow.

The mean momentum balance for channel flow is

$$\frac{\mathrm{d}^2U^+}{\mathrm{d}y^{+2}} + \frac{\mathrm{d}T^+}{\mathrm{d}y^+} + \epsilon^2 = 0. \tag{3.10}$$

The extra term $\epsilon^2 \equiv 1/\delta^+$ represents the dimensionless pressure gradient, and (3.4) is replaced by

$$T^+ = \frac{\mathrm{d}U^+}{\mathrm{d}y^+} = 0 \quad \text{at } \eta = 1. \tag{3.11}$$

In Couette flow, U^+ is odd about the point $\{\eta = 1, U^+ = U_c^+\}$ where U_c^+ is the centreline velocity (at $\eta = 1$). This means that $U^+(2-\eta) = 2U_c^+ - U^+(\eta)$, which results in a positive velocity $V^+ = 2U_c^+$ at the upper wall, $\eta = 2$. Also T^+ is even in the sense that $T^+(2-\eta) = T^+(\eta)$. In contrast, channel flow has $U^+(2-\eta) = U^+(\eta)$ and $T^+(2-\eta) = -T^+(\eta)$, which imply (3.11). Thus the two kinds of flow differ with respect to simple symmetry considerations.

There is, however, a deeper mathematical relation between them. In the Couette flow case, we can define an adjusted Reynolds stress

$$\tilde{T} \equiv T^+ - \epsilon^2 y^+. \tag{3.12}$$

Then (3.1) becomes

$$\frac{\mathrm{d}^2U^+}{\mathrm{d}y^{+2}} + \frac{\mathrm{d}\tilde{T}}{\mathrm{d}y^+} + \epsilon^2 = 0, \tag{3.13}$$

which in form coincides with (3.10). Thus, this simple transformation from T^+ to $\tilde{T}$ converts the differential equation for Couette flow to that for channel flow. Moreover, the boundary conditions satisfied by the variables in (3.13) turn out to be approximately the same as those satisfied by the corresponding variables in pressure-driven channel flow.

Qualitatively, the portion $\{0 < \eta < 1\}$ for Couette is analogous to a region close to the wall, $\{0 < \eta < \eta_m = O(\epsilon)\}$, for channel flow (Wei *et al.* 2005), where $\eta_m = O(\epsilon)$ is the location of the peak value of T^+. In both cases, T^+ rises to a maximum and U^+ rises to a point where $\mathrm{d}U^+/\mathrm{d}\eta$ has a smaller order of magnitude than it does at $\eta = 0$. That is, in both cases, the flow domain interior to the peak in T^+ constitutes a stress gradient balance layer. It will be shown that this observation leads to methodological similarities in describing other aspects of the two flows.

3.3. *Properties of T^+ and U^+ at the centreline*

Order of magnitude estimates for the magnitude of T^+ at the centreline, as well as for the curvature (flatness) of T^+ and U^+ will now be derived by scaling arguments.

Throughout the paper, the order symbol $O(\cdot)$ will be used with respect to $\epsilon \to 0$ or $\beta \to 0$ (β is a small parameter introduced in §3.4.1). For example, $a = O(b)$ for positive $a(\epsilon)$ and $b(\epsilon)$ will be taken to mean that a/b and b/a are both bounded for small ϵ.

Based on all empirical evidence, it may be assumed that for $0 < \eta < 1$

$$\left.\begin{aligned} &\frac{\mathrm{d}U^+}{\mathrm{d}y^+} > 0, \quad \frac{\mathrm{d}^2U^+}{\mathrm{d}y^{+2}} < 0 \quad \text{(Couette and channel)}, \\ &\frac{\mathrm{d}T^+}{\mathrm{d}y^+} > 0, \quad \frac{\mathrm{d}^2T^+}{\mathrm{d}y^{+2}} < 0 \quad \text{(Couette), the latter for } y^+ > \text{ a certain value.} \end{aligned}\right\} \tag{3.14}$$

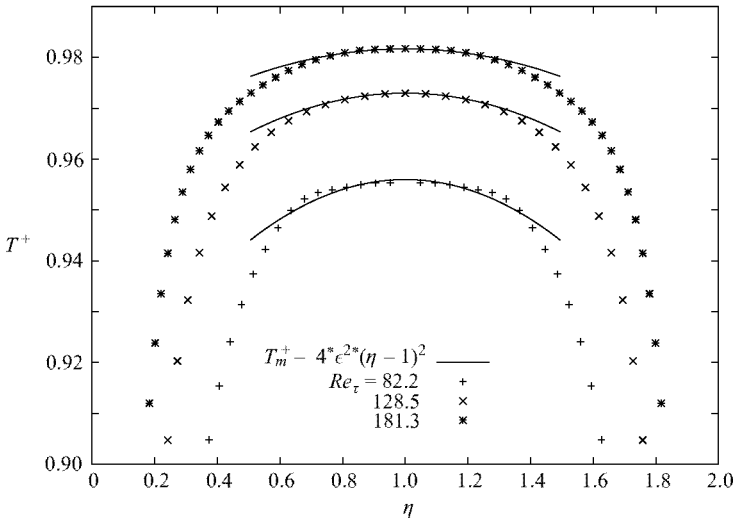

FIGURE 2. Reynolds stress around the peak, showing $\mathrm{d}^2T/\mathrm{d}\eta^2 = O(\epsilon^2)$ and $1 - T_m = O(\epsilon^2)$. Although these order of magnitude relations are clear, it is difficult to read off even the approximate value of $\mathrm{d}^2T/\mathrm{d}\eta^2$. The case $Re_\tau = 82$ is from DNS of Bech *et al.* (1995), and the other two cases are from DNS of Kawamura, Abe & Shingai (2000).

From this and (3.5), we see that for Couette flow, $T^+ < 1$ and that T^+ increases monotonically as we proceed from the lower wall to the centreline. Let $T_m^+ \equiv T_{\eta=1}^+$ be the maximal value of T^+. Recall the definition of $\hat{T}$ in (3.8), and (3.9). As mentioned, they suggest that near the centreline, both $\hat{T}$ and U^+ scale with η, in the sense that all their derivatives with respect to η are $\leqslant O(1)$ quantities. Further justification of this assertion will be provided in §3.4.6. In particular, $\mathrm{d}^2\hat{T}/\mathrm{d}\eta^2 \leqslant O(1)$, so that $\mathrm{d}^2T^+/\mathrm{d}\eta^2 \leqslant O(\epsilon^2)$. Therefore in that neighbourhood

$$T^+ \approx T_m^+ - K\epsilon^2(\eta - 1)^2,$$

for some K independent of ϵ, or

$$T^+ \approx T_m^+ - K\epsilon^6(y^+ - \delta^+)^2. \tag{3.15}$$

This provides the order of magnitude of the curvature of the T^+ profile at the centreline. Very good experimental support for this analytical prediction is given in figure 2, albeit only over a small range of Reynolds numbers.

Use of (3.6) at the centreline also provides the order of the deviation of T_m^+ from the value 1. Since it was noted above that η is the correct scaled variable for U^+ at the centreline, it is now seen that

$$T_m^+ = 1 - O(\epsilon^2). \tag{3.16}$$

Again, table 1 provides remarkable corroboration of (3.16).

In contrast, in pressure-driven turbulent channel flow, the proximity of T_m^+ to 1 is given by $T_m^+ = 1 - O(\epsilon)$, and the curvature of the graph of $T^+(y^+)$ is $O(\epsilon^3)$ near the peak (Wei *et al.* 2005). Table 2 provides a review of data corroborating the relation for channel flow. The contrast between the data of tables 1 and 2 is strong evidence of (3.16), despite the small range of Re_τ.

Investigators	Re_τ	T_m^+	$\dfrac{1-T_m^+}{\epsilon}$	$\dfrac{1-\boldsymbol{T}_m^+}{\epsilon^2}$
Bech *et al.*	82.2	0.955	0.4080	**3.699**
Kawamura *et al.*	128.5	0.9729	0.3066	**3.476**
Kawamura *et al.*	181.3	0.9817	0.2459	**3.311**

TABLE 1. Properties of T_m^+ for turbulent Couette flow. DNS data from Bech *et al.* (1995) and Kawamura *et al.* (2000).

Investigators	Re_τ	T_m^+	$\dfrac{1-\boldsymbol{T}_m^+}{\epsilon}$	$\dfrac{1-T_m^+}{\epsilon^2}$
Moser *et al.*	180	0.7321	**3.696**	49.321
Moser *et al.*	395	0.8370	**3.228**	69.935
Moser *et al.*	590	0.8647	**3.278**	79.447
Iwamoto *et al.*	109.4	0.6071	**4.110**	42.995
Iwamoto *et al.*	150.4	0.689	**3.815**	46.799
Iwamoto *et al.*	297.9	0.8006	**3.442**	59.401
Iwamoto *et al.*	395.7	0.8321	**3.340**	66.448
Iwamoto *et al.*	642.5	0.8746	**3.179**	80.574

TABLE 2. Properties of T_m^+ for turbulent channel flow. DNS data from Moser *et al.* (1999) and Iwamoto, Suzuki & Kasagi (2002).

Finally since $\mathrm{d}U^+/\mathrm{d}\eta \leqslant O(1)$ at $\eta = 1$,

$$\frac{\mathrm{d}U^+}{\mathrm{d}y^+} \leqslant O(\epsilon^2) \tag{3.17}$$

at $y^+ = \epsilon^{-2}$. Note that $\mathrm{d}^2U^+/\mathrm{d}\eta^2 = 0$ at $\eta = 1$, which illustrates that the actual order of derivatives of scaled quantities may be $\leqslant O(1)$ rather than $= O(1)$).

3.4. *The scale hierarchy*

The transformation (3.12), when generalized, leads to remarkable consequences regarding the structure of stress gradient balance layers. The foregoing scaling arguments, together with artificial adjusted Reynolds stresses, will be used systematically to reveal a continuum of scales, extending almost completely across the channel.

3.4.1. *Adjusted Reynolds stresses*

Let β be a small positive number. Restrictions on it will be given later. Let

$$T^\beta(y^+) = T^+(y^+) - \beta y^+. \tag{3.18}$$

(Note that β is a superscript not an exponent.) These are simply mathematical constructs that define the adjusted Reynolds stresses T^β. They satisfy

$$\frac{\mathrm{d}T^\beta}{\mathrm{d}y^+} = \frac{\mathrm{d}T^+}{\mathrm{d}y^+} - \beta, \tag{3.19}$$

and from (3.1) (as always, for Couette flow),

$$\frac{\mathrm{d}^2U^+}{\mathrm{d}y^{+2}} + \frac{\mathrm{d}T^\beta}{\mathrm{d}y^+} + \beta = 0. \tag{3.20}$$

From DNS data of Kawamura *et al.* (2000), the adjusted Reynolds stresses for different β are shown in figure 3.

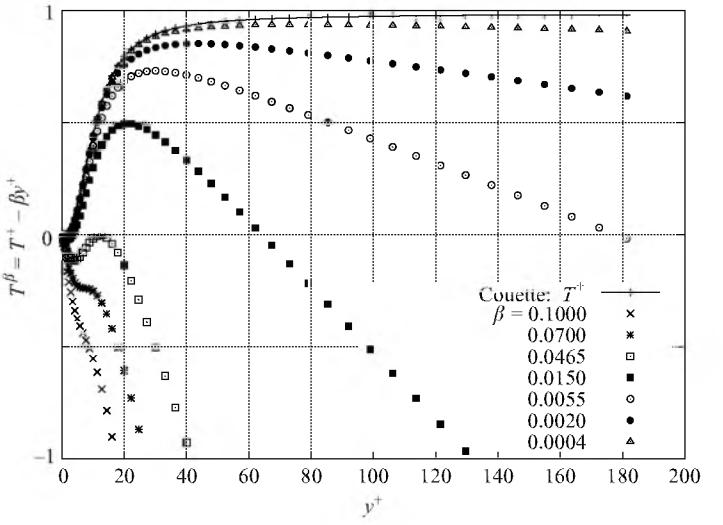

FIGURE 3. Adjusted Reynolds stress profile for various values of β. The case $\beta = \epsilon^4$ corresponds within $O(\epsilon^2)$ to the genuine Reynolds stress for Couette flow (see §3.4.6), and $\beta = \epsilon^2$ is an approximation to that for pressure-driven channel flow. The DNS data is from Kawamura *et al.* (2000), $\delta^+ = Re_\tau = 181.3$ and $\epsilon = 0.074$.

The main interest is in those adjusted stress functions that exhibit local maxima. This happens when β is sufficiently small. The reasoning in §3.5 uses these functions to educe the existence of a special scaling region (layer) L_β for each β in a certain range. Part of the argument involves obtaining an exact differential equation, (3.29), for rescaled variables having no explicit dependence on ϵ or β. Another part entails the recognition that (3.20) expresses an approximate balance between its first two terms (since β is small), and that this balance must be broken and changed to another kind of balance when y^+ attains a value such that the three terms in (3.20) have the same order of magnitude.

Balance-exchange occurs when β is such that there are locations $y^+ = y_0^+$ for which the middle term in (3.20) is positive and significantly greater than the last term. The actual balance-exchange will happen at slightly larger values of y^+, as shown below. Therefore we require $\mathrm{d}T^\beta/\mathrm{d}y^+(y_0^+) \gg \beta$. From (3.19), this will be the case when

$$\frac{\mathrm{d}T^+}{\mathrm{d}y^+}(y_0^+) \gg \beta. \tag{3.21}$$

Temporarily, (3.21) will be replaced by

$$\frac{\mathrm{d}T^+}{\mathrm{d}y^+}(y_0^+) \geqslant 10\beta. \tag{3.22}$$

Since this may be too restrictive, however, it will be relaxed at a later point by allowing the coefficient 10 to be changed to some number in the interval 5 to 20. Moreover, only points where $\mathrm{d}^2T^\beta/\mathrm{d}y^{+2} = \mathrm{d}^2T^+/\mathrm{d}y^{+2} < 0$ will be relevant, i.e. only points on the decreasing part of figure 4.

From figure 4, we see that $\max[\mathrm{d}T^+/\mathrm{d}y^+] \sim 0.07$, attained at $y^+ \sim 7$, so that (3.22) will be true for some y_0^+ if

$$0 < \beta \leqslant 0.007. \tag{3.23}$$

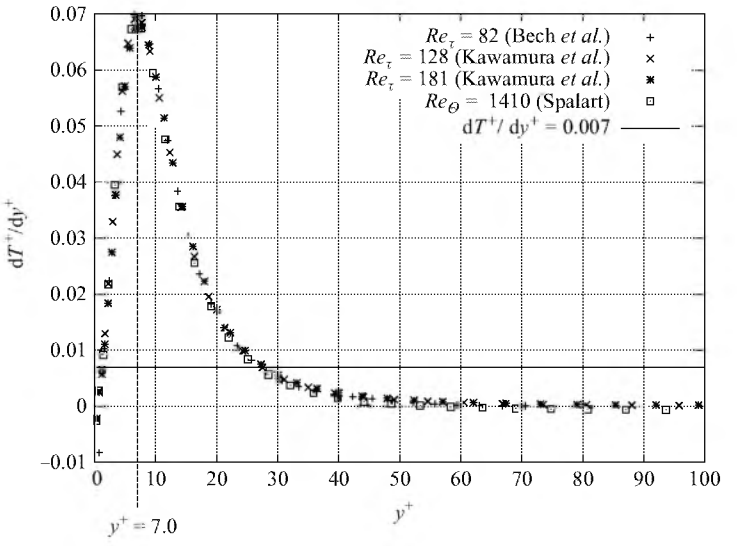

FIGURE 4. Inner normalized Reynolds stress gradient for a variety of flows. The turbulent Couette flow data are from Bech *et al.* (1995) and Kawamura *et al.* (2000). Also included are turbulent boundary layer DNS from Spalart (1988).

3.4.2. *Peaks of* T^β

Let β satisfy (3.23). There is a point on the right-hand (descending) branch of figure 4 at which $(dT^+/dy^+)(y^+) = \beta$, hence from (3.19) the function T^β has a maximum there (since its slope is 0 and its second derivative negative). Call the position of that maximum $y_m^+(\beta)$. As β decreases, y_m^+ increases toward its maximal allowed value, which is $1/\epsilon^2$ since that is the centreline. It will be shown in § 3.4.6 that $\beta = O(\epsilon^4)$ at the centreline.

A balance-exchange argument will be used to show that for each β satisfying (3.23) and $\beta \geqslant O(\epsilon^4)$, there exists a 'scaling layer' L_β with characteristic width $O(\beta^{-1/2})$ in the inner variable y^+, containing $y_m^+(\beta)$, such that in this layer, the functions U^+ and T^+ vary with characteristic length $\beta^{-1/2}$. It will also be shown that the characteristic width $\beta^{-1/2}$ is of the order of the actual layer position $y_m^+(\beta)$ as y_m^+ increases.

To reiterate, at the point $y_m^+(\beta)$ (where T^β is maximal), it follows from (3.19) that

$$\frac{dT^+}{dy^+}(y_m^+(\beta)) = \beta. \tag{3.24}$$

Hence since dT^+/dy^+ is a decreasing function of y^+, $y_m^+(\beta)$ increases as β decreases, with (as was mentioned in § 3.4.6) $y_m^+ \to 1/\epsilon^2$ as $\beta \to O(\epsilon^4)$. On the other hand, the range of β is limited, (3.23), by 0.007, and hence by figure 4, the lower bound on y_m^+ is about 30.

This provides a lower bound on the allowable values of y_m^+ which will be considered here as peaks in the graphs of T^β, with β subject to (3.22). Since the coefficient 10 in that inequality was quite arbitrary, it is worth exploring the consequences of replacing it by some number between 5 and 20. If that is done, it is found that the lower bound on y_m^+ is between 20 and 36.

In summary,

$$(20 \text{ to } 36) < y_m^+(\beta) < 1/\epsilon^2 \text{ when } (0.0035 \text{ to } 0.014) > \beta > O(\epsilon^4). \tag{3.25}$$

This range in y^+ will be the predicted range of the hierarchy, constructed below.

3.4.3. *A continuum of scalings*

It will be shown that within each layer L_β (to be defined below), the variables y^+ and T^β may be rescaled in such a way that the basic differential equation (3.20) is transformed into an exact equation having no explicit dependence on ϵ or β. This continuum of scales can be parameterized by either β or y_m^+, since $y_m^+(\beta)$ is a monotone function. It will be called a scale hierarchy. As will be shown and discussed further, there are compelling reasons to believe that scale hierarchies constitute a fundamental structural feature of the wall–turbulence equations; underlying, for example, the possible logarithmic behaviour of the mean profile, and replacing the traditional overlap ideas as the theoretical paradigm for that behaviour. The prediction that the beginning of the layered domain lies between $y^+ = 20$ and $y^+ = 36$ is interesting, in that it roughly coincides with the traditional empirical onset of the logarithmic-like profile. More generally, the striking connection between the hierarchy and the profiles of U^+ and T^+ is explored in § 3.5.

The details of the origin and properties of the layer L_β are now explained. Take β in the interval (3.23). Then (3.22) holds for some $y_0^+ < y_m^+(\beta)$. Therefore for $y^+ = y_0^+$, it follows from (3.22) that the first two terms in (3.20) are each much larger than the last term and balance, except for an error term β. This, in fact, continues to be true as y^+ increases to larger values, except that as y^+ approaches the location $y_m^+(\beta)$ where T^β achieves its maximum (denoted by $T_m^\beta(\beta)$) the middle term in (3.20) becomes smaller than $O(1)$, and therefore the first term does as well. The middle term eventually attains the value β (say) at some point, which will be called $y^+ = y_1^+(\beta)$. By (3.20), the first term $\mathrm{d}^2U^+/\mathrm{d}y^{+2} = -2\beta$ there. Therefore at $y^+ = y_1^+(\beta)$, all three terms in (3.20) have the same order of magnitude, and it is natural to seek a rescaling which reflects this equality. The new variables will be called $\hat{y}$ (which also depends on β) and $\hat{T}^\beta$. As exemplified in Wei *et al.* (2005), rescaling is best done using the differentials, $\mathrm{d}y^+$ and $\mathrm{d}T^\beta$. For coefficients α and γ, to be determined depending on β, we set

$$\mathrm{d}y^+ = \alpha\,\mathrm{d}\hat{y}, \quad \mathrm{d}T^\beta = \gamma\,\mathrm{d}\hat{T}^\beta. \tag{3.26}$$

Under this transformation, the first two terms in (3.20) become $\alpha^{-2}\mathrm{d}^2U^+/\mathrm{d}(\hat{y})^2$ and $(\gamma/\alpha)(\mathrm{d}\hat{T}^\beta/\mathrm{d}\hat{y})$ respectively. They must match, in formal order of magnitude, the third term, β. This requires $\alpha = \beta^{-1/2}$ and $\gamma = \beta^{1/2}$. Therefore

$$\mathrm{d}y^+ = \beta^{-1/2}\,\mathrm{d}\hat{y}, \quad \mathrm{d}T^\beta = \beta^{1/2}\,\mathrm{d}\hat{T}^\beta. \tag{3.27}$$

The equations (3.27) can be integrated with integration constants chosen such that $\hat{y} = 0$ when $y^+ = y_m^+(\beta)$ and $\hat{T}^\beta = 0$ when $T^\beta = T_m^\beta(\beta)$:

$$y^+ = y_m^+(\beta) + \beta^{-1/2}\hat{y}, \quad T^\beta = T_m^\beta + \beta^{1/2}\hat{T}^\beta. \tag{3.28a, b}$$

The basic equation (3.20) then becomes

$$\frac{\mathrm{d}^2U^+}{\mathrm{d}\hat{y}^2} + \frac{\mathrm{d}\hat{T}^\beta}{\mathrm{d}\hat{y}} + 1 = 0. \tag{3.29}$$

This is an exact equation with no explicit dependence on any parameters, and it suggests that the β-dependent rescaling just described, (3.28), accurately depicts the behaviour of U^+ and $\hat{T}^\beta$ (hence T^+) in some 'scaling patch', but that evidence is not quite sufficient. It should also be independently demonstrated that at some location in the channel, the individual derivatives appearing in (3.29) are actually $\leqslant O(1)$ quantities. Then the existence of a scaling patch containing that location can

be surmised. In the patch, U^+ and $\hat{T}^\beta$ will be regular functions of $\hat{y}$, which means in particular that the derivatives of those functions (to orders 1, 2 and 3, say) with respect to $\hat{y}$ will also be $O(1)$ quantities. There are, in fact, two candidates for such a location: $y_1^+(\beta)$ and $y_m^+(\beta)$. For example by construction, at $y_1^+(\beta)$ the terms of (3.29) are -2, 1 and 1, respectively. This, together with the fact that y_1^+ is not at a boundary, where external influences could occur, is evidence of the presence of a local 'scaling layer' L_β containing that point. In other words, the characteristic length scale in this interval, referred to the variable $\hat{y}$, has the order unity, and thus by (3.28) in wall units is $O(\beta^{-1/2})$.

The other candidate is the point $y_m^+(\beta)$ where the three terms in (3.29) are $-1, 0$ and 1, respectively. The layer L_β will contain both points, but the latter, $y_m^+(\beta)$, will be chosen in this paper to pinpoint the layer. In view of (3.28*a*), the characteristic length ℓ^+ in the layer can be taken as $\ell^+ = \beta^{-1/2}$.

At this point, it has been shown that for each value of β in the range (3.25), there exists an interval L_β containing $y_m^+(\beta)$ (and $y_1^+(\beta)$) within which U^+ and $\hat{T}^\beta$ are regular functions of $\hat{y}$, hence with reference to the inner variable y^+, these functions vary with characteristic length $\beta^{-1/2}$.

The 'width' of L_β in the inner variable y^+ can then be surmised as being $O(\beta^{-1/2})$, although its width is not a well-defined concept, since L_β overlaps with nearby layers ($L_{\beta'}$, for β' near β.) Since $y_1^+(\beta)$ and $y_m^+(\beta)$ are in L_β, some corroboration of its magnitude being $O(\beta^{-1/2})$ may be obtained by estimating $y_m^+(\beta) - y_1^+(\beta)$, which by (3.28) is $\Delta y^+ = \beta^{-1/2}\Delta\hat{y}$, $\Delta\hat{y} = 0 - \hat{y}_1$. The corresponding increment in $\mathrm{d}^2U^+/\mathrm{d}\hat{y}^2$ is

$$\Delta\frac{\mathrm{d}^2U^+}{\mathrm{d}\hat{y}^2} = -1 - (-2) = 1.$$

However, for some value $\hat{y}^*$ in layer L_β, the mean value theorem says that the left-hand side $= (\mathrm{d}^3U^+/\mathrm{d}\hat{y}^3)(\hat{y}^*)\Delta\hat{y}$, so that $\Delta\hat{y} = (\mathrm{d}^3U^+/\mathrm{d}\hat{y}^3)^{-1}$. By differentiating (3.29), it is seen that $\mathrm{d}^3U^+/\mathrm{d}\hat{y}^3 = -\mathrm{d}^2\hat{T}^\beta/\mathrm{d}\hat{y}^2$. This derivative, evaluated at $\hat{y} = 0$ ($y^+ = y_m^+(\beta)$) will be called

$$A(\beta) = -\frac{\mathrm{d}^2\hat{T}^\beta}{\mathrm{d}\hat{y}^2}(0), \tag{3.30}$$

although it depends also (probably weakly except for β values corresponding to maxima near the centreline) on ϵ. It is the curvature of the peak in T^β, in locally scaled coordinates, so that $A(\beta) > 0$. It will be shown below in § 3.4.4 that $A(\beta) = O(1)$ for all β. Therefore $\Delta\hat{y} = 1/A = O(1))$ as well. This corroborates the characteristic width $\Delta y^+ = O(\beta^{-1/2})$ found before.

If β_1 and β_2 are close to each other, L_{β_1} and L_{β_2} overlap. However, a discrete set of values of β may be chosen so that the associated layers do not overlap, but nevertheless fill out the entire domain of the hierarchy (3.25). If this is done, the number of members in the ensemble increases indefinitely as $\epsilon \to 0$.

In summary, layer L_β is characterized in part by the characteristic length (in inner units) of variation of U^+ and T^+ being $O(\beta^{-1/2})$ and

$$\mathrm{d}U^+/\mathrm{d}\hat{y} = O(1), \quad \mathrm{d}U^+/\mathrm{d}y^+ = O\big(\beta^{1/2}\big), \tag{3.31}$$

the higher derivatives of $\mathrm{d}U^+/\mathrm{d}\hat{y}$ and $\hat{T}$ are $\leqslant O(1)$.

Its location will be considered in § 3.4.4.

This process, by which the layer L_β appears, involves a breaking of the approximate balance of the first two terms in (3.20) as y^+ increases past a critical value y_1^+, and

its replacement by a balance among all three terms in (3.20), as indicated formally by (3.29). However, the middle term of (3.29) soon vanishes (at $y^+ = y_m^+(\beta)$), resulting in a balance between the first and third terms alone. This breaking and reestablishing of a balance can be called a 'balance exchange'. It plays a very prominent role in the scaling analysis of turbulent channel flow (Wei *et al.* 2005), and as shown here is an embedded property of stress gradient balance layers.

The above constitutes the theoretical foundation for the scale hierarchy. Namely, it provides the existence of a layer L_β, for each value of β in the interval $O(\epsilon^4) < \beta <$ (a value between 0.0035 and 0.014), located at $y_m^+(\beta)$. There will be considerable overlapping of layers. This translates into the range of y_m^+ given by (3.25).

An important question remains as to how the unadjusted Reynolds stress T^+ scales in L_β. The answer comes from (3.18): $T^+ = T^\beta + \beta y^+ = T_m^\beta + \beta y_m^+ + \beta^{1/2}(\hat{T}^\beta + \hat{y}) = T_m^\beta + \beta y_m^+ + \beta^{1/2}\hat{T}_*(\hat{y})$, where this expression defines $\hat{T}_*(\hat{y}) = \hat{T}^\beta(\hat{y}) + \hat{y}$. It is a regular function of $\hat{y}$. Therefore the conclusion is that in L_β, T^+ also scales with $\hat{y}$. In fact

$$T^+ = T_m^\beta + \beta y_m^+ + \beta^{1/2}\hat{T}_*, \tag{3.32}$$

where $\hat{T}_*$ is a regular function of $\hat{y}$ (i.e. its derivatives are bounded independently of ϵ or β). Of course, U^+ is also a regular function of $\hat{y}$ in L_β. This result is self-consistently reinforced by the fact that (3.32) is analogous to the rescaling derived in (3.28).

3.4.4. *Locations of the layers*

An important piece of information is still lacking. This relates to how the location $y_m^+(\beta)$ (which serves to pinpoint L_β) of the maximum of T^β depends on β. Once this is found, the behaviour of the velocity $U^+(y^+)$ and the Reynolds stress $T^+(y^+)$ can in principle be obtained. It is shown, in fact, that for large $y_m^+(\beta)$, the characteristic extent of the layer has the order of magnitude of its distance $y_m^+(\beta)$ from the wall. This means that the layer occupies a fraction of the distance y^+ from the wall to the centre of the layer itself.

By differentiating (3.24) with respect to β, we obtain

$$\frac{\mathrm{d}^2 T^+}{\mathrm{d}y^{+2}}(y_m^+(\beta))\frac{\mathrm{d}y_m^+}{\mathrm{d}\beta} = 1. \tag{3.33}$$

This equation holds for all y_m^+ for which $y_m^+(\beta)$ is defined, and in particular for all y_m^+ given by (3.25). Also by (3.27)

$$\frac{\mathrm{d}^2 T^+}{\mathrm{d}y^{+2}} = \beta^{1/2}\frac{\mathrm{d}^2 T^+}{\mathrm{d}y^+\mathrm{d}\hat{y}} = \beta\frac{\mathrm{d}^2 T^+}{\mathrm{d}\hat{y}^2} = \beta^{3/2}\frac{\mathrm{d}^2 \hat{T}^\beta}{\mathrm{d}\hat{y}^2}. \tag{3.34}$$

In L_β, derivatives such as $\mathrm{d}^2\hat{T}^\beta/\mathrm{d}\hat{y}^2$ are $O(1)$ quantities (independent of ϵ to dominant order). Recall (3.30) $A = -(\mathrm{d}^2\hat{T}^\beta/\mathrm{d}\hat{y}^2)_{\hat{y}=0}$; then $A = O(1)$ (see below). Although A will generally depend on β, i.e. on y_m^+, its order of magnitude will not change. From (3.34),

$$\frac{\mathrm{d}^2 T^+}{\mathrm{d}y^{+2}} = -A(y_m^+)\beta^{3/2}. \tag{3.35}$$

Putting this into (3.33) gives

$$\frac{\mathrm{d}y_m^+}{\mathrm{d}\beta} = -\frac{1}{A}\beta^{-3/2}. \tag{3.36}$$

Since $A(\beta) = O(1)$, it satisfies bounds of the form $0 < \alpha_1 < 1/A < \alpha_2$, and from (3.36), there is a C independent of β with $y_m^+(\beta) = C - \int (1/A)\beta^{-3/2}\,\mathrm{d}\beta$, so that

$$2\alpha_1\beta^{-1/2} + C < y_m^+(\beta) < 2\alpha_2\beta^{-1/2} + C. \tag{3.37}$$

In short, $y_m^+(\beta) = O(\beta^{-1/2})$ $(\beta \to 0)$, and since $\beta^{-1/2}$ is the characteristic length in L_β, this establishes the claim that the characteristic length of L_β is asymptotically proportional to its distance $y_m^+(\beta)$ from the wall.

It is appropriate here to discuss further the issue of the constancy of the order of magnitude of $A(\beta)$. It was shown that the rescaled variables belonging to each member of the scaling hierarchy satisfy (3.29) exactly (no approximation). The parameters β and ϵ do not appear in that equation (except implicitly in the definitions of the rescaled variables). Therefore although the definitions (3.28) of the rescaled variables $\hat{y}$ and $\hat{T}^\beta$ depend on β (3.28), the equation they satisfy does not. This suggests that in each scaling patch the functions $U^+(\hat{y})$ and $\hat{T}^\beta(\hat{y})$, of the β-dependent variable $\hat{y}$ would be invariant (approximately) when β changes, i.e. would enjoy some β-independence when evaluated at the same value of $\hat{y}$ within the various different scaling patches. This would hold as well for their derivatives. This conclusion is given more credence, in fact, by the observation that at the point $y^+ = y_m^+(\beta)$, i.e. at $\hat{y} = 0$, each term appearing in (3.29) has a value $(-1, 0, 1)$, respectively, independent of β, and the undifferentiated quantity $\hat{T}^\beta = 0$ does as well. It is to be concluded that $A(\beta) = O(1)$ for all β, and that there may be circumstances when the function A itself is almost constant.

3.4.5. *Determination of $U^+(y^+)$ from A*

Knowledge of the characteristic function $A(\beta)$ of the hierarchy would lead rigorously and uniquely, up to integration constants, to the profiles of U^+ and T^+. This is done by integrating (3.36), (3.24) and (3.5), which are written here in terms of the general coordinate $y^+ = y_m^+$ in the hierarchy, representing the location of the maximal point of T^β:

$$\frac{\mathrm{d}y^+}{\mathrm{d}\beta} = -\frac{1}{A(\beta)}\beta^{-3/2}, \tag{3.38}$$

$$\frac{\mathrm{d}T^+}{\mathrm{d}y^+} = \beta, \tag{3.39}$$

$$\frac{\mathrm{d}U^+}{\mathrm{d}y^+} = 1 - T^+. \tag{3.40}$$

Integration of (3.38) yields $y^+ - C$ as a function of β, where C is an integration constant which can be determined by fitting a known value of y^+ with its known value of β. Inverting that function gives β as a function of $y^+ - C$. Integrating (3.39) and then (3.40) finally provides T^+ and U^+. As mentioned, the resulting function U^+ is logarithmic if and only if $A = \text{constant}$.

3.4.6. *The case $\beta = \epsilon^4$*

Here it is shown that the traditional outer scaling $\eta = \epsilon^2 y^+$ fits into the hierarchy at $\beta = \epsilon^4$, and that it is the proper scaling to use near the centre of the flow $(\eta = 1)$, as was asserted below (3.9). It is seen from (3.27) that in the case $\beta = \epsilon^4$

$$\mathrm{d}\hat{y} = \epsilon^2\,\mathrm{d}y^+ = \mathrm{d}\eta, \tag{3.41}$$

so that $\hat{y}$ and η differ only in their origins:

$$\hat{y} = \eta - \eta_m, \tag{3.42}$$

where η_m is defined as the value of η where $T^{(\beta=\epsilon^4)}$ has its maximum. Therefore it is to be expected that $\eta = 1$ is in the layer $L_{\beta=\epsilon^2}$. In fact, the order of magnitude of $1 - \eta_m$ can be found. At that point, the left-hand side of (3.19) $= 0$, and by differentiating (3.15), the right-hand side $\sim 2K\epsilon^6(1/\epsilon^2 - y_m^+) - \epsilon^4$. The graphs in figure 2 suggest that $K \sim 4$. Therefore $1/\epsilon^2 - y_m^+ \sim (1/8)\epsilon^{-2}$, i.e.

$$1 - \eta_m \sim 1/8. \tag{3.43}$$

Empirical data show, in fact, that $1 - \eta_m \sim 0.1$.

In summary, when $\beta = \epsilon^4$, the location of the maximum adjusted Reynolds stress $T^{(\beta=\epsilon^4)}$ lies within a distance of about 0.1 (in η, i.e. in $\hat{y}$ for this value of β) of the maximum of T^+ itself, which is at $\eta = 1$. Thus for $\beta = \epsilon^4$, except for a small shift of the order ~ 0.1, $\hat{y}$ and η are identical scaled distances. Thus the centreline $\eta = 1$ lies in the layer $L_{\beta=\epsilon^2}$, where U^+ and $\hat{T}^\beta = (T^\beta - T_m^\beta)/\epsilon^2$ (3.28) are regular functions of η. This corroborates the assertion to that effect following (3.9).

3.5. *The question of logarithmic-type growth*

A central issue in the history of turbulent channel flow investigations is whether and where the mean velocity profile exhibits a logarithmic growth. The approach adopted in this paper provides new insight into this issue. The first conclusion to be reached is that logarithmic profiles of U^+ depend crucially on $A(\beta)$ (§ 3.4.4) being constant. If it is constant, then exact logarithmic growth follows easily from the calculations below. If it is not constant, then the growth is not logarithmic. If A is almost constant (and reasons for supposing that it is so under certain circumstances are given), then the profile of U^+ is bounded between two nearby logarithmic functions. Finally in § 3.5.2, a non-rigorous argument is presented leading to the conclusion that as $Re \to \infty$, A approaches a constant in certain moving ranges (characterized explicitly) of y^+ values.

3.5.1. *The issue of the constancy of* $A(\beta)$

The reasoning following (3.37) and below in § 3.5.2 indicates that A may be approximately constant for values of y_m^+ far from the limits of its allowed range (3.25). For now, suppose that $A =$ constant in some interval. From (3.38), we find

$$y_m^+ = C + \frac{2}{A}\beta^{-1/2}, \quad \beta = \frac{4}{A^2}(y^+ - C)^{-2}, \tag{3.44}$$

and hence from (3.39),

$$\frac{\mathrm{d}T^+}{\mathrm{d}y^+}(y_m^+) = (2/A)^2(y_m^+ - C)^{-2}. \tag{3.45}$$

Replacing y_m^+ by the general variable y^+ and integrating,

$$T^+(y^+) = C' - (2/A)^2(y^+ - C)^{-1}. \tag{3.46}$$

Since $T^+ \to 1$ as $y^+ \to \infty$ (this is only possible in the limit $\epsilon \to 0$), the constant $C' = 1$.

Putting this into (3.5) yields

$$\frac{\mathrm{d}U^+}{\mathrm{d}y^+} = 1 - T^+ = (2/A)^2(y^+ - C)^{-1}. \tag{3.47}$$

Integrating again,

$$U^+(y^+) = (2/A)^2 \ln(y^+ - C) + C'', \tag{3.48}$$

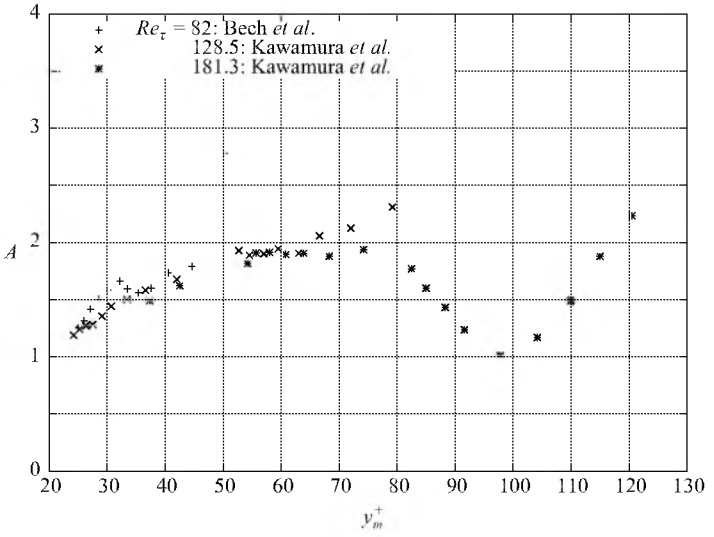

FIGURE 5. $A(y^+)$ for different Reynolds numbers as estimated by finite difference of $T^+(y^+)$. These estimates indicate a trend to larger internal intervals of relatively constant A for larger Re, thus agreeing with the present theory. The total range of the function A also increases with Re. The values of A were calculated from finite differencing DNS data of Bech *et al.* (1995) and Kawamura *et al.* (2000), (3.35), with locations y_m^+ determined from figure 3.

providing logarithmic growth with a 'von Kármán constant' $\kappa = A^2/4$. Although the usual logarithmic law lacks the constant C, an additive adjustment of this type has been proposed both by the studies of George & Castillo (1997) and Oberlack (2001).

The conclusions (3.48) and (3.46) were under the assumption that A = constant. That assumption of constancy is unlikely ever to be exactly true. However, the trend shown in the computed values of A in figure 5 (unknown accuracy) suggests that for large Re, $A(\beta)$ may be 'relatively' constant in interior regions of its range. An extreme case is discussed in § 3.5.2.

The effect of an approximate constancy of A on the validity of (3.46) and (3.48) can be easily seen. Write the dependence of A on β as dependence on $y_m^+ = y_m^+(\beta)$, i.e. $A = A(y_m^+(\beta))$. Suppose that the function $A(y_m^+)$ has a range lying in the interval $A_0 - \sigma \leqslant A(y_m^+) \leqslant A_0 + \sigma$ for some constant A_0 and some small positive number σ. Then (3.36) becomes a pair of inequalities which bound the left-hand side inside an interval depending on σ. The integration steps (3.45)–(3.48) then result in inequalities of the form

$$1 - (c_0 + \sigma c_1)(y^+ - C)^{-1} \leqslant T^+ \leqslant 1 - (c_0 - \sigma c_1)(y^+ - C)^{-1}, \tag{3.49}$$

$$(c_2 - \sigma c_3)\ln(y^+ - C) \leqslant U^+ - C'' \leqslant (c_2 + \sigma c_3)\ln(y^+ - C). \tag{3.50}$$

3.5.2. *A limiting situation*

In the hierarchy, each y^+ can be identified as being a point $y_m^+(\beta)$ for some β. The corresponding β will be called $\beta(y^+)$. In this way, each y^+ has a layer $L_{\beta(y^+)}$ containing y^+, such that $-A(\beta)$ is the scaled second derivative of T^β at its peak. What mechanism will cause $A(\beta)$ to vary? Certainly not the mean momentum balance partial differential equation, (3.29), in that vicinity, nor the values of the scaled derivatives $\mathrm{d}\hat{T}^\beta/\mathrm{d}\hat{y} = 0$ or $\mathrm{d}^2U^+/\mathrm{d}\hat{y}^2 = -1$ (from (3.29)) at that peak location, because these things do not change with β. The only source for such a variation would be influence from neighbouring

layers. Extending that chain of influence, we could speak, on the one hand, of the influence due to layers $L_{\beta'}$ lower in the hierarchy with $\beta' > \beta$, stretching down to those values of y^+ at or near the lower limit of the hierarchy, i.e. the smallest values of y^+ which accommodate a layer, $y^+ \sim 20$ to 36, (3.25). It stands to reason that this influence of the lower part of the hierarchy will diminish as it becomes more remote, i.e. as the original y^+ becomes large.

A similar chain of influence extends toward higher values of y^+, i.e. $\beta' < \beta$, capped only by the upper bound $y^+ = \epsilon^{-2}$, at or near the centreline. The centreline, however, becomes further, as $\epsilon \to 0$, from the original point y^+ if the latter is fixed or moves outward as $\epsilon \to 0$ more slowly than ϵ^{-2}.

Consider, then, a band of values of y^+, depending on ϵ, which migrate away from the wall (measured in the wall coordinate y^+) as $\epsilon \to 0$, but more slowly than ϵ^{-2}. An example would be the intermediate band $\{\epsilon^{-1/2} < y^+ < \epsilon^{-3/2}\}$. In that interior band, the above argument suggests that the values of A will become more and more independent of any influence from the upper and lower limits of the hierarchy, and therefore would tend to become constant. In the limit as $\epsilon \to 0$, therefore, the analysis relating to the case A = constant would apply so that (3.46) and (3.48) would be approached in that band.

3.6. *Summary*

These arguments verify that for each y^+ in the range

$$(\text{a value between 20 and 36}) < y^+ \leqslant 1/\epsilon^2, \tag{3.51}$$

there is a layer L_β with $y^+ = y_m^+(\beta)$, where $\hat{y}$ and $\hat{T}^\beta$ are the proper scaled variables for distance and adjusted Reynolds stress $\hat{T}^\beta$, (3.18). The characteristic length in this layer is $O(1)$ in the scaled variable $\hat{y}$, and $O(\beta^{-1/2})$ in y^+. Thus for small enough β, the characteristic length coincides in order of magnitude with its position y^+. In regions where A is approximately constant, logarithmic-type growth, (3.49) and (3.50), holds.

4. Turbulent channel flow induced by a pressure gradient

The purpose of this section is to illustrate that scale hierarchies exist in pressure-driven flow. In fact, the evidence below indicates why these hierarchies not only comprise the stress gradient balance layer, but the entire flow domain of the traditionally defined logarithmic layer.

4.1. *Previous analytical results*

The following is a summary of the main findings contained in Wei *et al.* (2005). Each of these results is in accord with the scaling analysis in that paper and the data compiled there from past experimental and DNS sources. We use the same notation, such as $y^+, \eta, U^+, T^+, \delta^+, \epsilon$, as Wei *et al.* The averaged mean momentum equation is (3.10), with boundary conditions (3.2) and (3.11).

The channel is divided into four principal layers with the properties described in § 2.

The Reynolds stress profile has the following features. The function T^+ vanishes with its derivative at $y^+ = 0$, increases monotonically with y^+ to a maximum value $T_m^+ = 1 - O(\epsilon)$ at a point $y_m^+ = O(1/\epsilon)$, and then slowly decreases, approaching the value 0 in a linear fashion as $\eta \to 1$. The expression for T^+ in this latter region is

$$T^+(\eta) = 1 - \eta + O(\epsilon^2). \tag{4.1}$$

In a vicinity of the maximum, the function $T^+(y^+)$ has the behaviour

$$T^+(y^+) \sim T_m^+ - C\epsilon^3(y^+ - y_m^+)^2. \tag{4.2}$$

The mesolayer constitutes a region in which $|y^+ - y_m^+| \leqslant O(1/\epsilon)$. In it, the profiles are properly described in terms of $\hat{T}$ and U^+ as functions of $\hat{y}$, where $T^+ = T_m^+ + \epsilon\hat{T}(\hat{y})$ and $y^+ = y_m^+ + \epsilon^{-1}\hat{y}$.

4.2. *Hierarchy*

To exhibit a hierarchy of layers in the channel-flow profile, all that is needed is to revise slightly the definition of the adjusted Reynolds stresses, (3.18). The new one is defined by

$$T^\beta(y^+) = T^+(y^+) + \epsilon^2 y^+ - \beta y^+. \tag{4.3}$$

This transforms the basic momentum balance equation, (3.10), into

$$\frac{\mathrm{d}^2U^+}{\mathrm{d}y^{+2}} + \frac{\mathrm{d}T^\beta}{\mathrm{d}y^+} + \beta = 0, \tag{4.4}$$

which is of the same form as (3.20).

Therefore, with the newly adjusted Reynolds stresses, the channel-flow context is amenable to the balance exchange processes described in § 3.4.1, the construction of a continuum of scalings with associated layers L_β in § 3.4.3, and (under some assumptions) the derivation of logarithmic-like profiles in § 3.5. The scaling in L_β is still given by (3.27).

The mean profile calculations are given here only for the simplest case $A =$ constant, although analogues of (3.38)–(3.40) can be derived. As before, the expressions (3.36) and (3.35) are obtained in the present setting as well; but the integration of (3.35) yields a different integration constant. It is required that $\mathrm{d}T^+/\mathrm{d}y^+ = 0$ at $y^+ = y_m^+$, the location of the maximum of the original unadjusted T^+. Therefore (3.45) is replaced, under the same supposition that $A =$ constant, by

$$\frac{\mathrm{d}T^+}{\mathrm{d}y^+}(y^+) = (2/A)^2[(y^+ - C)^{-2} - (y_m^+ - C)^{-2}], \tag{4.5}$$

where now the variable y^+ is the same variable as in (3.46) and y_m^+ was just defined. Note that this derivative changes sign as y^+ passes through y_m^+, as it should. Integrating once again, we obtain

$$T^+(y^+) = C' - (2/A)^2(y^+ - C)^{-1} - (2/A)^2(y_m^+ - C)^{-2}y^+. \tag{4.6}$$

However, there is now a known boundary condition, $T^+ = 0$ at $y^+ = 1/\epsilon^2$; this serves to determine the constant C'.

Similar to the previous procedure, we may now use the integrated form of (3.10) to determine $\mathrm{d}U^+/\mathrm{d}y^+$ and integrate it with the boundary conditions that the derivatives of U^+ vanish as $y^+ \to \infty$ to obtain the same log dependence as in (3.48):

$$U^+(y^+) = (2/A)^2 \ln(y^+ - C) + C''. \tag{4.7}$$

Again, this is all under the (doubtful) assumption that A is exactly constant. In the case that it is almost constant, we obtain a pair of bounds like (3.50), valid now for the mean velocity in channel flow for the range of y^+ constructed as before. Note that in the case $\beta = \epsilon^2$, by (4.3), $T^\beta = T^+$.

4.3. *The mesolayer*

When $\beta = \epsilon^2$, the adjusted Reynolds stress T^β, (4.3), coincides with the actual Reynolds stress T^+, so that the corresponding layer $L_{\beta=\epsilon^2}$ will be located near the location of the maximum of T^+. As mentioned in §4.1, this is how the mesolayer III was identified in Wei *et al.* (2005).

Each of the layers L_β can be thought of as an adjusted mesolayer, constructed by replacing the actual T^+ by T^β. In this sense, the actual mesolayer $L_{\beta=\epsilon^2} = \text{III}$ is just one among many. It is distinguished, however, on the one hand as the location where the actual Reynolds stress reaches its maximum and its gradient changes sign, and on the other hand as the location where an important force balance exchange takes place.

4.4. *The outer layer and the extent of the hierarchy*

When $\beta = \epsilon^4$, it follows as before from (3.27) that $\mathrm{d}y^+ = \epsilon^{-2}\mathrm{d}\hat{y} = \epsilon^{-2}\mathrm{d}\eta$, so that outer scaling holds and $L_{\beta=\epsilon^4}$ is in the outer region, far beyond y_m^+. The range of the hierarchy therefore extends well beyond the traditional 'log layer'.

5. Summary and discussion

Theoretical tools of multiscale analysis were shown in Wei *et al.* (2005) to be useful in elucidating the structure of fully developed pressure-driven turbulent channel flow found, in the same paper, by an examination of empirical data. That structure consists of four primary layers, one of them being a stress gradient balance layer, wherein the gradients of the viscous and Reynolds stresses balance, to within a very good approximation.

The analogous fully developed turbulent Couette flow consists of only the stress gradient balance layer, since those two gradients provide the only forces internal to the flow. In the present paper, the range of applicability of the same multiscale techniques was shown to be much greater than shown in Wei *et al.* (2005). Applied to Couette flow, they reveal a mathematical structure in which the mean axial velocity and Reynolds stress exhibit a hierarchy of characteristic lengths and corresponding layers (in a sense secondary to the primary stress gradient balance layer) covering the major part of the flow domain. Other important information is also found, such as:

(i) The characteristic lengths are asymptotically proportional to distance between the wall and the layer (they are reminiscent of, but different from, the mixing lengths of Prandtl (Prandtl 1925; von Kármán 1930).

(ii) There is a rigorous connection between the $O(1)$ function $A(\beta)$, defined explicitly in terms of the layer hierarchy, and the mean velocity and Reynolds stress profiles.

(iii) The U^+ profile is logarithmic in an interval only if $A = \text{constant}$ in that same interval; there is evidence, theoretical and computational, that it is relatively constant in some intervals in some cases. However, the focus of the paper has been more on offering explanations and reasons for important phenomena than on obtaining numerical information.

(iv) The range of values of y^+ at which the layered region begins is predicted, and matches the empirical location of the onset of the traditional logarithmic profile.

(v) Order of magnitude properties of the Reynolds stress profile near the centreline (its curvature and the deviation of its maximum from 1) are found.

Another important finding is that a simple transformation, applied to the Reynolds stress, provides the way to transfer almost all of this information to the analogous

pressure-driven turbulent flow. Namely, in the latter setting there is also a hierarchy of scales and layers with properties (i)–(iv) (properties (v) were obtained in Wei *et al.* 2005).

The hierarchical layer structure is associated with *exchange of balance* phenomena very similar to that used to reveal the properties of the mesolayer in Wei *et al.* (2005). The generalization in this paper used 'adjusted Reynolds stresses'.

The success of theoretical tools applied only to the Reynolds-averaged momentum balance equation may be surprising, since the equation is not closed, underdetermined, and therefore not capable of supplying an exact solution. Along with the analysis, some crucial, but minimal, assumptions of an essentially physical nature were required. The existence of a correct scaling of the variables with its concomitant scaling layer was in each case surmised by showing (i) that it leads to a differential equation which, to leading order, expresses a force balance between at least two of the three terms in an adjusted conservation of momentum equation, and (ii) that at some location, the terms in that differential equation are, when properly scaled, each $O(1)$ in magnitude. These criteria for the existence of a layer, in fact, also form the theoretical basis for the traditional inner and outer scalings. Other useful information, gleaned from empirical data, are that the mean velocity and Reynolds stress profiles are monotone increasing in distance from the lower wall, with their slopes decreasing beyond a certain point.

Overall, the formulations herein provide considerable information relative to the mathematical structure of the equations governing wall-turbulence. An overarching element of this analysis is the manner by which the terms in the momentum equation undergo the exchange of balance just mentioned. As shown regarding the fundamental layer structure of pressure-driven channel flow by Wei *et al.* (2005) and herein with regard to the continuum of layers constituting the scale hierarchy, the particular exchange of balance phenomenon under consideration (others may occur under different flow configurations) takes place across a Reynolds-number-dependent layer and is characterized by specific scaling behaviours derivable from the properties of the momentum equation within this layer. For the pressure-driven flow equation employing the unadjusted Reynolds stress, this physically represents a transition from mean flow dynamics characterized by a balance between the viscous and Reynolds stress gradient to dynamics described by a balance involving all three forces, and on to a balance between the Reynolds stress gradients and the mean axial pressure gradient. For the members of the scale hierarchy (described by equations containing the adjusted Reynolds stresses), the physical interpretation is less clear cut. In either case, however, the flow field decomposition resulting from exchange of balance mathematics is retained as a property intrinsic to the structure of the mean flow equations. The implications of these conclusions are significant with regard to both modelling and theoretical considerations.

For example, since the mean flow equations have been shown inherently to contain a hierarchical layer structure, hierarchy-based models (e.g. Townsend 1976; Perry & Chong 1982; Perry & Marusic 1995; Kerstein 1999) would seem to have natural advantages. That is, irrespective of the details of any given model, the hierarchical property alone would probably yield a relatively high degree of efficacy. It is relevant to note that the results of § 3.4.3 revealed that for large (inner) distance, the distance from the wall is a length scale embodied in the composition of the scale hierarchy. While the distance from the wall is often invoked as a characteristic length in turbulent wall layers (e.g. Townsend 1976; Schlichting & Gersten 2000), its use relies on physical arguments that are not necessarily supported by observations. Perhaps

the most common assertion in this regard is that the scale of the largest eddy near the wall is well represented by the distance from the wall. Measures of the scale of the vorticity bearing motions, however, do not lend direct support for such an assertion (Klewicki & Falco 1996). Indeed, the series of recent results from the University of Illinois and elsewhere (see below) indicate a significantly more complex situation in which instantaneous agglomerations of eddies (i.e. packets) collectively exhibit a distance from the wall scaling. Independent of empirical evidence, the present results provide theoretical justification for the distance from the wall as a characteristic length that is founded in the mathematical structure of the mean momentum balance. As revealed herein, this property comes about non-trivially through the structure of the scale hierarchy.

The mathematics underlying the mean momentum balance layer structure and the embedded scale hierarchy argue quite strongly against the appropriateness of the classical overlap ideas (as outlined in § 1) for describing the mean velocity profile. That is, while consequences of overlap ideas have obviously been empirically verified to provide a useful framework for curve-fitting the data, the present analyses indicate that a conceptual framework in the form of outer and inner domains, plus something else in between, is contrary to the actual structure, in which the inner and outer scales are simply two extremes in a spectrum of scaling domains. The discussion is first clarified by noting that the inner/outer matching procedure described by Izakson (1937) and Millikan (1939) must be supplemented by the restrictive additional physical assumption that the mean velocity profile is strictly increasing with distance from the wall. Generic examples, however, show that this is an unusual occurrence among two-scale problems. Another generic class of examples (discussed in the cited paper) questions the hypothesis that there even exists a domain of overlap. Moreover, in the case of Couette flow, simultaneously satisfying an outer (inertial) functional form and an inner (viscous) one is not conceptually consistent with the fact that the entire flow constitutes a stress gradient balance layer. Similarly, in boundary-layer and pressure-driven channel flow the empirical and theoretical evidence given herein and in Wei *et al.* (2005) show that, according to the mean momentum balance, the traditionally defined overlap layer actually contains all or part of three (principal) layers described by distinctly different dynamics. On the other hand, the exchange of balance property elucidated herein not only describes the layer-to-layer transitions and the internal structure of stress gradient balance layers, but also analytically predicts the existence of a generalized logarithmic-like variation in the mean profile. Specifically, in § 3.5 it was shown that under some circumstances the scale hierarchy naturally leads to mean profile variations close to logarithmic functions. These inequalities are, to date, believed to constitute the most theoretically well-founded bounds for the shape of the mean profile.

Given the loss of information associated with time averaging, these may in fact be the most that can be said with much theoretical rigour. It is important to note that the inexactness expressed by these bounds no doubt allows Reynolds-number dependence, and both 'logarithmic' and some limited power law forms to be fit between the bounds. Thus, even though the ideas of Izakson and Millikan yield conclusions which are generally consistent with those obtained here, overlapping function mathematics have little connection to either mean flow dynamics or to the origin of the logarithmic-like behaviour of the mean profile.

Lastly, while the scale hierarchy is born from the mathematics associated with the structure of the time-averaged equations of motion, speculative connections to the instantaneous motions in turbulent wall flows are worthy of brief mention. In particular,

recent detailed particle image velocimetry (PIV) measurements provide mounting evidence that organized packets of hairpin-like vortices are an important (arguably irreducible) element of the instantaneous structure of boundary layers (Meinhart & Adrian 1994; Adrian, Meinhart & Tomkins 2000; Christensen & Adrian 2001; Ganapathisubramani, Longmire & Marusic 2003; Tomkins & Adrian 2003). Key attributes of these vortex packets have intriguing similarities to the scale hierarchy, including: (i) an embedded hierarchical structure, (ii) linear scale growth with distance from the wall, and (iii) a distinct velocity increment embedded within each level of the vortex packet structure. While these similarities may simply be coincidence, the identification of an instantaneous connection to the time-averaged structure of the governing equations would constitute an enormous advance. For this reason, further investigation and experiments (especially at higher Reynolds numbers) are felt to be warranted.

This work was supported by the US Department of Energy through the *Centre for the Simulation of Accidental Fires and Explosions* under grant W-7405-ENG-48, the National Science Foundation under grant CTS-0120061 (grant monitor, M. Plesniak), and the Office of Naval Research under grant N00014-00-1-0753 (grant monitor, R. Joslin). The authors thank K. H. Bech, N. Tillmark, P. H. Alfredsson and H. Andersson; R. D. Moser, J. Kim and N. N. Mansour; K. Iwamoto, Y. Suzuki and N. Kasagi (http://www.thtlab.t.u-tokyo.ac.jp/DNS/); and H. Kawamura, H. Abe and K. Shingai (http://murasun.me.noda.tus.ac.jp/db/DNS.html) for supplying their DNS data; and M. Buschmann, M. Gad-el-Hak and R. L. Panton for discussions relating to some of these issues.

REFERENCES

Adrian, R. J., Meinhart, C. D. & Tomkins, C. D. 2000 Vortex organization in the outer region of the turbulent boundary layer. *J. Fluid Mech.* **422**, 1–54.

Afzal, N. 1984 Mesolayer theory for turbulent flows. *AIAA J.* **22**, 437–439.

Afzal, N. 1993 Asymptotic analysis of turbulent Couette flow. *Fluid Dyn. Res.* **12**, 163–171.

Afzal, N. 2001*a* Power law and log law velocity profiles in fully developed turbulent boundary layer flow: equivalent relations at large Reynolds number. *ACTA Mech.* **151**, 195–216.

Afzal, N. 2001*b* Power law and log law velocity profiles in fully developed turbulent pipe flow: equivalent relations at large Reynolds number. *ACTA Mech.* **151**, 171–183.

Bech, K. H., Tillmark, N., Alfredsson, P. H. & Andersson, H. I. 1995 An investigation of turbulent plane Couette flow at low Reynolds numbers. *J. Fluid Mech.* **304**, 285–319.

Buschmann, M. H. & Gad-el-Hak, M. 2003*a* Debate concerning the mean-velocity profile of a turbulent boundary layer. *AIAA J.* **41**, 565–572.

Buschmann, M. H. & Gad-el-Hak, M. 2003*b* Generalized logarithmic law and its consequences. *AIAA J.* **41**, 40–48.

Christensen, K. T. & Adrian, R. J. 2001 Statistical evidence of hairpin vortex packets in wall turbulence. *J. Fluid Mech.* **431**, 433–443.

DeGraaff, D. B. & Eaton, J. K. 2000 Reynolds-number scaling of the flat-plate turbulent boundary layer. *J. Fluid Mech.* **422**, 319–346.

Gad-el-Hak, M. & Bandyopadhyay, P. R. 1994 Reynolds number effects in wall-bounded turbulent flows. *Appl. Mech. Rev.* **47**, 307–365.

Ganapathisubramani, B., Longmire, E. K. & Marusic, I. 2003 Characteristics of vortex packets in turbulent boundary layers. *J. Fluid Mech.* **478**, 35–46.

George, W. K. & Castillo, L. 1997 Zero-pressure-gradient turbulent boundary layer. *Appl. Mech. Rev.* **50**, 689–729.

Gill, A. E. 1968 The Reynolds number similarity argument. *J. Maths Phys.* **47**, 437–441.

Hinze, J. O. 1975 *Turbulence*, 2nd edn. McGraw–Hill, New York.

IWAMOTO, K., SUZUKI, Y. & KASAGI, N. 2002 Reynolds number effect on wall turbulence: toward effective feedback control. *Intl J. Heat Fluid Flow* **23**, 678–689.

IZAKSON, A. 1937 On the formula for the velocity distribution near walls. *Tech. Phys. USSR* **IV**, **2**, 155.

KÁRMÁN, VON T. 1930 Mechanische Ahnlichkeit und Turbulenz. *Nachr. Ges. Wiss. Gottingen, Math-Phys. Klasse*, pp. 58–76.

KAWAMURA, H., ABE, H. & SHINGAI, K. 2000 DNS of turbulence and heat transport in a channel flow with different Reynolds and Prandtl numbers and boundary conditions. In *Turbulence, Heat and Mass Transfer 3 (Proc. of the 3rd Intl Symp. on Turbulence, Heat and Mass Transfer)*, pp. 15–32. Aichi Shuppan.

KERSTEIN, A. R. 1999 One-dimensional turbulence: model formulation and application to homogeneous turbulence, shear flows and buoyant stratified flows. *J. Fluid Mech.* **392**, 277–334.

KLEWICKI, J. C. & FALCO, R. E. 1996 Spanwise vorticity structure in turbulent boundary layer. *Intl J. Heat and Fluid Flow* **17**, 363–376.

LONG, R. R. & CHEN, T.-C. 1981 Experimental evidence for the existence of the mesolayer in turbulent systems. *J. Fluid Mech.* **105**, 19–59.

MCKEON, B. J., MORRISON, J. F., LI, J., JIANG, W. & SMITS, A. J. 2004 Further observations on the mean velocity in fully-developed pipe flow. *J. Fluid Mech.* **501**, 135–147.

MEINHART, C. D. & ADRIAN, R. J. 1994 On the existence of uniform momentum zone in a turbulent boundary layer. *Phys. Fluids* **7**, 694–696.

MILLIKAN, C. B. 1939 A critical discussion of turbulent flows in channel and circular tubes. In *Proc. of the Fifth International Congress of Applied Mechanics* (ed. J. P. D. Hartog & H. Peters), pp. 386–392. Wiley.

MONIN, A. S. & YAGLOM, A. M. 1971 *Statistical Fluid Mechanics*, 1st edn. MIT Press.

MOSER, R. D., KIM, J. & MANSOUR, N. N. 1999 Direct numerical simulation of turbulent channel flow up to $Re_\tau = 590$. *Phys. Fluids* **11**, 943–945.

OBERLACK, M. 2001 A unified approach for symmetries in plane parallel turbulent shear flows. *J. Fluid Mech.* **427**, 299–328.

PANTON, R. L. 1990 Scaling turbulent wall layers. *Trans. ASME* I: *J. Fluids Engng* **112**, 425–432.

PANTON, R. L. 1997 A Reynolds stress function for wall layers. *Trans. ASME* I: *J. Fluids Engng* **119**, 325–330.

PANTON, R. L. 2005 Review of wall turbulence as described by composite expansions. *Appl. Mech. Rev.* (To appear).

PERRY, A. E. & CHONG, M. S. 1982 On the mechanism of wall turbulence. *J. Fluid Mech.* **119**, 173–217.

PERRY, A. E. & MARUSIC, I. 1995 A wall–wake model for the turbulence structure of boundary layers. Part 1. Extensions of the attached eddy hypothesis. *J. Fluid Mech.* **298**, 361–388.

POPE, S. B. 2000 *Turbulent Flow*, 1st edn. Cambridge University Press.

PRANDTL, L. 1925 Bericht uber die Entstehung der Turbulenz. *Z. Angew. Math. Mech.* **5**, 136–139.

SCHLICHTING, H. & GERSTEN, K. 2000 *Boundary Layer Theory*, 8th edn. Springer.

SPALART, P. R. 1988 Direct simulation of a turbulent boundary layer up to $Re_\theta = 1410$. *J. Fluid Mech.* **187**, 61–98.

SREENIVASAN, K. R. & SAHAY, A. 1997 The persistence of viscous effects in the overlap region, and the mean velocity in turbulent pipe and channel flows. In *Self-Sustaining Mechanisms of Wall Turbulence* (ed. R. Panton), pp. 253–272. Computational Mechanics Publications, Southampton, UK.

TENNEKES, H. & LUMLEY, J. L. 1972 *First Course in Turbulence*, 1st edn. MIT Press.

TOMKINS, C. D. & ADRIAN, R. J. 2003 Spanwise structure and scale growth in turbulent boundary layers. *J. Fluid Mech.* **490**, 37–74.

TOWNSEND, A. A. 1976 *The Structure of Turbulent Shear Flow*, 2nd edn. Cambridge University Press.

WEI, T., FIFE, P., KLEWICKI, J. & MCMURTRY, P. 2005 Properties of the mean momentum balance in turbulent boundary layer, pipe and channel flows. *J. Fluid Mech.* **522**, 303–327.

ZAGAROLA, M. V. & SMITS, A. J. 1997 Scaling of the mean velocity profile for turbulent pipe flow. *Phys. Rev. Lett.* **78**, 239–242.